Development 134, 2925-2933 (2007) doi:10.1242/dev.001925

Spatiotemporal definition of neurite outgrowth, refinement and retraction in the developing mouse cochlea

Lin-Chien Huang[1], Peter R. Thorne[2], Gary D. Housley[1,*] and Johanna M. Montgomery[1,†]

The adult mammalian cochlea receives dual afferent innervation: the inner sensory hair cells are innervated exclusively by type I spiral ganglion neurons (SGN), whereas the sensory outer hair cells are innervated by type II SGN. We have characterized the spatiotemporal reorganization of the dual afferent innervation pattern as it is established in the developing mouse cochlea. This reorganization occurs during the first postnatal week just before the onset of hearing. Our data reveal three distinct phases in the development of the afferent innervation of the organ of Corti: (1) neurite growth and extension of both classes of afferents to all hair cells (E18-P0); (2) neurite refinement, with formation of the outer spiral bundles innervating outer hair cells (P0-P3); (3) neurite retraction and synaptic pruning to eliminate type I SGN innervation of outer hair cells, while retaining their innervation of inner hair cells (P3-P6). The characterization of this developmental innervation pattern was made possible by the finding that tetramethylrhodamine-conjugated dextran (TMRD) specifically labeled type I SGN. Peripherin and choline-acetyltransferase immunofluorescence confirmed the type II and efferent innervation patterns, respectively, and verified the specificity of the type I SGN neurites labeled by TMRD. These findings define the precise spatiotemporal neurite reorganization of the two afferent nerve fiber populations in the cochlea, which is crucial for auditory neurotransmission. This reorganization also establishes the cochlea as a model system for studying CNS synapse development, plasticity and elimination.

KEY WORDS: Cochlea, Afferent nerve fibers, Neurite, Peripherin, ChAT, Neuronal tracer, Tetramethyl rhodamine dextran, Hearing, Mouse

INTRODUCTION

The development of the mammalian nervous system involves a number of synchronous events, including neurite growth towards appropriate targets, the formation of new synaptic connections, plasticity to reapportion synaptic contacts and axon retraction to remove inappropriate innervation and synapses (Malenka, 2003; Oster and Sretavan, 2003; Walsh and Lichtman, 2003; Montgomery and Madison, 2004; Sugihara, 2006). In the developing cochlea, these events are likely to play a crucial role in establishing the correct afferent innervation pattern. In the cochlea, sensory hair cells transduce the acoustic signal. The tonotopic organization of the sensory epithelium (the organ of Corti) and the intensity-dependent hair cell depolarization determine the firing of the spiral ganglion neurons (SGN), the primary auditory neurons (Pickles, 1988). This primary afferent innervation of the hair cells is complex, with two functionally distinct neuron populations conveying sound information to the central auditory system. Each of the approximately 800 inner hair cells (IHC) in the adult mouse cochlea are exclusively innervated by up to 20 type I SGNs (approximately 95% of the total neuron population) and are the principal encoders of the auditory signal. By contrast, the approximately 2600 outer hair cells (OHC) share an en passant innervation by type II SGN (approximately 5% of the neuron population) (Keithley and Feldman, 1982; Burda and Branis, 1988; Slepecky, 1996; Pujol et al., 1998). Type II SGN innervation is likely to provide sensory feedback from the OHC region as part of a neural control loop within the central auditory nuclei that includes inhibitory olivocochlear efferent innervation of both the OHC and the postsynaptic region of the type I SGN at the IHC (Pickles, 1988; Jagger and Housley, 2003; Darrow et al., 2006; Darrow et al., 2007).

Before the cochlear afferent innervation reaches this mature configuration, there is an initial mismatch, where both populations of SGN innervate both types of sensory hair cells: during the first postnatal week in the rodent cochlea, type I SGN innervation is eliminated from the OHC and type II SGN innervation is eliminated from the IHC (Perkins and Morest, 1975; Echteler, 1992; Simmons, 1994). One major obstacle to defining neurite retraction and synaptic remodeling in the cochlea has been the inability to distinguish the origin of the nerve fibers either before or during neurite retraction from the mismatched hair cells. Previous studies have revealed the overall pattern of axonal growth in the cochlea using electron microscopy, Golgi staining, horseradish peroxidase histochemistry and lipophilic dyes to label SGN and trace the nerve fibers to the hair cell region during development (Perkins and Morest, 1975; Echteler, 1992; Simmons, 1994; Bruce et al., 1997). However, it has not been possible to unequivocally identify the SGN subtypes until neurite reorganization was complete. For the first time, we have independently tracked the development of the two SGN populations in the mouse cochlea using tetramethylrhodamine-conjugated dextran (TMRD) to label type I SGN and peripherin immunolabeling to identify type II SGN. This has enabled us to directly visualize the time frame and the dynamics of the developing afferent innervation patterns and precisely define the spatiotemporal reorganization of auditory neurites that precedes the onset of hearing.

MATERIALS AND METHODS

Animals

All procedures in this study were approved by the University of Auckland Animal Ethics Committee. Cochleae were obtained from embryonic day 18 (E18), postnatal day 0-12 (P0-P12) and adult (P35-P42) C57/BL6 mice. The

[1]Department of Physiology and [2]Section of Audiology, Faculty of Medical and Health Sciences, University of Auckland, Private Bag 92019, Auckland, New Zealand.

*Present address: Department of Physiology, Faculty of Medicine, University of New South Wales, Sydney, Australia
†Author for correspondence (e-mail: jm.montgomery@auckland.ac.nz)

Accepted 7 June 2007

cochleae were surgically removed after the mice were killed with an overdose of sodium pentabarbitone (90 mg/kg; Nembutal, Virbac Laboratories, New Zealand) by intraperitoneal injection.

Neuronal tracer application

The neuronal tracer TMRD (3000 Da MW, anionic and lysine fixable, Molecular Probes, USA) moves along nerve processes in the antero- and retrograde direction largely via diffusion (Gimlich and Braun, 1985; Glover et al., 1986; Popov and Poo, 1992; Fritzsch, 1993; Kaneko et al., 1996; Kobbert et al., 2000). TMRD is hydrophilic, enabling fast dye uptake into the axoplasm of the cut nerve fibers, and exhibits high signal efficacy compared with other fluorochrome-conjugated dextrans. Previous studies have shown TMRD to provide significant resolution of nerve terminal structures and a high specificity of labeling (Glover et al., 1986; Fritzsch, 1993; Kaneko et al., 1996; Kobbert et al., 2000). Therefore TMRD was utilized to identify the innervation patterns of nerve processes in the developing cochlea. TMRD of 3 kDa was chosen because of its faster diffusion rate compared with larger molecular weight dextrans. The most prominent advantage of this tracer arose from a fortuitous observation of ours: when TMRD was applied to the freshly cut eighth cranial (vestibulocochlear) nerve, it was transported within minutes to the neuronal cell bodies that had neurites projecting as radial fibers solely to the IHC. The specific labeling of neonatal type I SGN by TMRD was substantiated by the results of this developmental study.

The medial surface of the auditory bulla and the internal auditory meatus were exposed by sectioning the cranium in the sagittal plane and removing the brain. TMRD crystals were manually applied with fine forceps to the vestibulocochlear nerve bundle at the internal auditory meatus and incubated at room temperature for 20 minutes [modified from Boyer et al. (Boyer et al., 2004)]. To remove excess dye crystals, the tissue was rinsed with artificial cerebrospinal fluid [aCSF; 130 mM NaCl, 3 mM KCl, 2 mM $CaCl_2$, 1.3 mM NaH_2PO_4, 2 mM $MgSO_4$, 20 mM glucose, 20 mM $NaHCO_3$, 0.4 mM ascorbic acid, pH 7.4]. Cochleae were dissected and incubated at room temperature for 4 hours in aerated or oxygenated (carbogen 95% O_2 and 5% CO_2) aCSF. Temperature and incubation time were optimized from multiple trials: the incubation time was optimized according to the diffusion rate [2 mm/hour at 22°C for 3 kDa dextran (Fritzsch, 1993)], the travel distance of TMRD in the nerve fibers from the internal auditory meatus to the apical region through the spiral ganglion neurones to the nerve terminals (~4 mm in P0-P6 mouse), and the time required to attain the maximum signal at the nerve terminals through the turns without tissue degradation from autolysis (see Fig. S1 in the supplementary material). Incubation times of less than 4 hours resulted in a weaker signal in the nerve terminals in the mid and apical regions. Increasing the incubation temperature to 37°C accelerated tissue autolysis. Therefore, our parameters for dextran application to the cochlea are believed to provide the optimal results for both signal intensity and tissue integrity. Cochleae were subsequently perfused with 4% paraformaldehyde in 0.1 M phosphate buffer (pH 7.4) through the round and oval windows and post-fixed overnight.

Immunocytochemistry

Immunocytochemistry enabled identification of type II SGN and cholinergic efferent fibers using the antibodies against peripherin and choline acetyltransferase (ChAT), respectively (Sobkowicz and Emmerling, 1989; Hafidi, 1998). Peripherin is a 57 kDa type III intermediate filament protein that in the rat cochlea is found only in type II SGN (Hafidi, 1998) and has been used extensively as a specific marker for type II SGN (Hafidi et al., 1993; Despres et al., 1994; Mou et al., 1998; Schimmang et al., 2003). Peripherin polyclonal rabbit antiserum (PII/SE411) against rat peptide sequence IETRDGEKVVTESQKEQHSELDKSSIHSY was a gift from Dr Annie Wolff (Djabali et al., 1991; Terao et al., 2000). Choline acetyltransferase (ChAT) polyclonal goat antibody (Chemicon) identified cholinergic efferent fibers in the cochlea (Sobkowicz and Emmerling, 1989).

For whole-mount preparations, the spiral ligament, Reissners' membrane and tectorial membrane were removed to ensure antibody penetration. The apical, mid and basal regions of the cochlea were dissected separately to permit the study of spatial differences in innervation patterns. In addition, some cochleae were processed as floating sections. In these cases, cochleae were cryoprotected with 10% sucrose in 0.1 M PBS for 4 hours, then 30% sucrose in PBS overnight, followed by incubation in 30% sucrose and Tissue-Tek (OCT, Miles, IN) (1:1) for 1 hour. Cochleae were then mounted in OCT, frozen in dry ice and cryosectioned (CM1900 cryostat microtome, Leica, Germany) at 50 μm thickness into 0.1 M PBS.

Whole mounts or cross-sections were incubated in a blocking/permeabilizing solution at 4°C for 1 hour [10% normal goat or horse serum (NGS or NHS; Vector Laboratories, CA), and 1% Triton X-100 in 0.1 M PBS] and then incubated at 4°C overnight in primary antibody solution: anti-peripherin antibody (1:800 in 5% NGS in 0.1% Triton X-100 in 0.1 M PBS) for peripherin immunolabeling; anti-ChAT antibody (1:200 in 5% NHS in 0.1% Triton X-100 in 0.1 M PBS) for ChAT immunolabeling. Alexa 488-conjugated goat anti-rabbit IgG or Alexa 647-conjugated donkey anti-goat IgG (1:500; Molecular Probes), were applied at room temperature (2 hours), then incubated at 4°C (2 hours). After washes, the tissues were mounted on glass slides (Vectashield, Vector Laboratories) and stored at 4°C. Omission of primary antibodies in negative controls resulted in no signal (data not shown). The specificity of peripherin expression in type II SGN was validated in previous studies (Djabali et al., 1991; Hafidi et al., 1993; Despres and Romand, 1994; Mou et al., 1998; Terao et al., 2000). We further confirmed the specificity of our peripherin antibody by successfully reproducing peripherin expression patterns in the neonatal rat cochlea as described by Hafidi et al. (Hafidi et al., 1993) (see Fig. S2 in the supplementary material).

Image acquisition and analysis

Images were acquired via confocal microscopy (Leica TCS SP2, Germany, or Olympus FV1000, Japan) and processed using Adobe Photoshop software. Maximal intensity projections of stacks of optical sections were used to resolve labeled nerve fibers within cochlear sections and whole mounts (Leica confocal software or Olympus FV10-ASW 1.3). Three-dimensional reconstruction using ~25 optical sections provided additional resolution of the afferent innervation pattern (Image Pro Plus 3D suite, Media Cybernetics, MD, USA). Unless otherwise stated, data presented here are from the mid-turn of the cochlea. This enabled a comparison of innervation patterns across developmental stages independent of the basal-to-apical cochlea maturation gradient (Ruben, 1967; Lenoir et al., 1980; Roth and Bruns, 1992a; Roth and Bruns, 1992b; Pujol et al., 1998).

RESULTS

Postnatal day 6 afferent innervation patterns approach the mature cochlear configuration

Significant neurite and synapse remodeling occurs to establish the mature innervation pattern of the cochlea. At P6 we found that the cochlear afferent innervation pattern was representative of the mature neural organization (Fig. 1). TMRD labeled the majority of SGN cell bodies within Rosenthal's canal in the apical, mid and basal turns of the cochlea (Fig. 1 and see Fig. S1 in the supplementary material). Labeled neurites extending from these cells projected as radial fibers to the inner spiral plexus region beneath the row of IHC in the apical, mid and basal turns (Fig. 1 and see Fig. S1 in the supplementary material). Peripherin-positive type II SGN cell bodies formed a distinct subpopulation primarily localized on the outer edge of the spiral ganglion adjacent to the (efferent) intraganglionic spiral bundle. TMRD labeling was clearly independent of peripherin-labeled type II SGNs (Fig. 1), indicative that TMRD was selectively labeling type I SGN fibers. Few type II SGNs occurred among the majority of TMRD-positive type I SGNs in the mid-cochlea level (Fig. 1). Unlike type I SGNs, peripherin-immunolabeled type II SGNs were absent in the most apical region, but towards the mid and basal turn the number of peripherin-expressing fibers in the outer spiral bundles gradually increased, similar to the type II SGN distribution that has been previously described (Keithley and Feldman, 1979; Hafidi et al., 1993). The peripherin-positive neurites arising from the type II SGNs projected

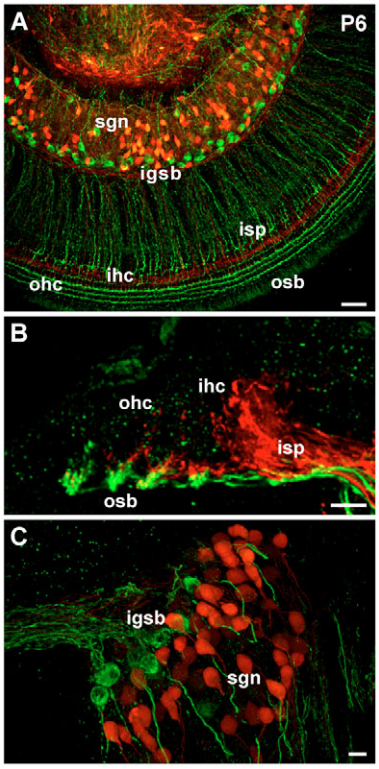

Fig. 1. Double labeling of TMRD and peripherin distinguished the adult-like innervation pattern of the type I and type II SGN afferent neurite projections within the P6 mouse cochlea. Maximum intensity projection of confocal images demonstrate the independent labeling of the type I and type II SGN by TMRD (red) and peripherin immunofluorescence (green), respectively. TMRD-labeled fibers in the intraganglionic spiral bundles, running around the perimeter of Rosenthal's canal, are consistent with TMRD also labeling the efferent fibers at this mature stage (see Fig. 6). The SGN cell bodies and their associated neurites innervating the hair cells are shown in whole mounts (**A**) and in cross sections (**B**,**C**). (A) Overview of basal turn of the cochlea. (B,C) Details of the sensory hair cell region and the spiral ganglion in the mid-turn of the cochlea. (B) TMRD-labeled neurites innervating the inner hair cells at inner spiral plexus, with additional neurites extending towards outer hair cells. The type I fibers traveled above the peripherin-expressing type II fibers. The latter bypassed the IHC region and traveled along the basilar membrane to form three rows of outer spiral bundles, which innervated the OHCs. (C) TMRD and peripherin immunofluorescence labeled the type I and type II SGNs, respectively. TMRD-labeled neurons were distributed throughout the ganglion, while peripherin-labeled neurons were found close to the intraganglionic spiral bundles. Scale bars: 50 μm in A; 10 μm in B,C. igsb, intraganglionic spiral bundles; ihc, inner hair cells; isp, inner spiral plexus; ohc, outer hair cells; osb, outer spiral bundles.

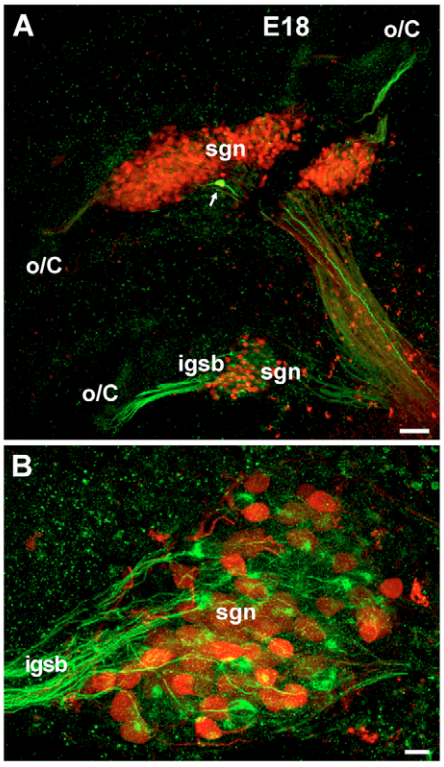

Fig. 2. TMRD and peripherin labeling in the E18 mouse cochlea. (**A**) An overview of TMRD (red) and peripherin (green) labeling in the cochlea shows that the TMRD-labeled type I neurons were found in both the apical and the mid-turn regions, while peripherin expression in the type II neurons was higher in the mid turn. In this example, peripherin was strongly expressed in a single neuron located close to the modiolus in the apical turn (arrow). (**B**) TMRD and peripherin labeling was independent in the SGN. The peripherin-expressing neurons were scattered throughout the ganglion. Scale bars: 50 μm in A; 10 μm in B. igsb, intraganglionic spiral bundle; isp, inner spiral plexus; osb, outer spiral bundles.

alongside the type I radial fibers to the IHC region, but then passed beneath the tunnel of Corti and established three rows of basally traversing fibers, the outer spiral bundles, beneath the rows of OHC and Deiters' cells (Hafidi et al., 1993; Hafidi, 1998).

3D confocal image reconstructions showed that the TMRD-labeled radial fibers passed above the peripherin-labeled outer spiral fibers in the osseous spiral lamina and inner spiral plexus regions (Fig. 1B, Fig. 5F; see Movie S2 in the supplementary material). The terminals of the TMRD-labeled type I SGN radial fibers were localized to the basolateral region of the IHC and extended further up the lateral wall of the IHC on their medial aspect (Fig. 1B, Fig. 4G,I, Fig. 5D,F, Fig. 6N,Q). Peripherin labeled outer spiral fibers were evident between Deiters' cells, but the labeling was absent at the terminals on the OHC (Fig. 1B, Fig. 4H,I, Fig. 5E,F). Analysis of P12 and adult cochlea (not shown) confirmed that the P6 tissue reflected the mature differential afferent organization.

Establishment of cochlear afferent innervation

Independent labeling of the type I and type II SGNs by TMRD and peripherin enabled us to visualize and characterize the development of cochlear dual afferent innervation patterns. As noted, presentation of data is primarily from the mid-turn region of the cochlea to avoid the confounding complexity of the base-apex maturation gradient (Ruben, 1967; Lenoir et al., 1980; Pujol et al., 1998; Roth and Bruns, 1992a; Roth and Bruns, 1992b).

From E18 to P6, the neurite fiber tracts innervating the IHCs and OHCs showed no overlapping labeling with TMRD and peripherin. At E18, TMRD labeling of SGNs was evenly dispersed throughout all turns of the spiral ganglion (Fig. 2A). Peripherin immunolabeling was found in a subgroup of neurons throughout all turns, with expression increasing in the mid and basal turn regions (Fig. 2). In comparison to P6, the peripherin-positive type II SGNs at E18 were more numerous and were not restricted to the region close to the

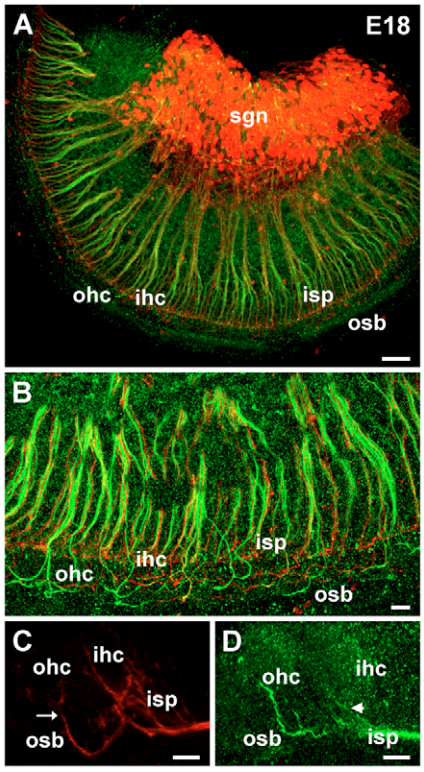

Fig. 3. Immature cochlear afferent innervation pattern at E18 in mice. (**A**) An overview of TMRD (red; type I SGNs) and peripherin (green; type II SGNs) labeling in a whole-mount preparation displayed as a maximum intensity projection. (**B**) TMRD- and peripherin-labeled neurites in the organ of Corti exhibited an unorganized innervation pattern under the OHCs. These neurites traveled only a short distance in the outer spiral bundles (OSBs). TMRD labeling was also found under the IHCs. (**C**,**D**) Organ of Corti cross section from a single confocal optical section provides an alternative view under the hair cells. (C) TMRD-labeled neurites in the inner spiral plexus region, showing innervation of the IHCs. Type I fibers also traveled along the basilar membrane to innervate the first row of OHCs via the OSBs (arrow). (D) Peripherin-expressing neurites traveled along the basilar membrane, and entered the OSBs to target an OHC. Peripherin-expressing fibers also formed collateral innervation to the IHCs via thin fibers (arrowhead). Scale bars: 50 μm in A; 10 μm in B; 20 μm in C,D. isp, inner spiral plexus; osb, outer spiral bundles.

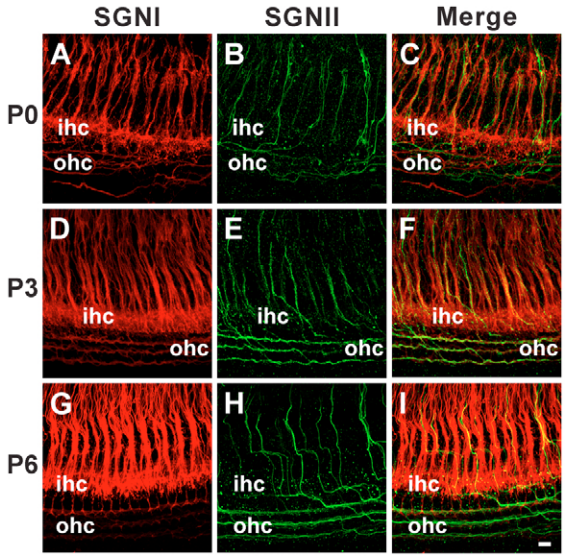

Fig. 4. Development of the afferent innervation in the cochlea during neurite reorganization (P0-P6) in mice. TMRD- and peripherin-labeled neurites undergo refinement (P0-P3) and retraction (P3-P6), as demonstrated by maximum intensity projections of confocal images from cochlear whole-mount preparations. (**A**,**D**,**G**) TMRD labeling (red) of type I afferent nerve fibers. These neurites innervate the IHCs between P0 and P6. Peripherin (green) immunolabeling of type II afferent nerve fibers (**B**,**E**,**H**) and merged images (**C**,**F**,**I**) demonstrate the independence and the relationship between TMRD and peripherin labeling. (A-C) At P0, both TMRD- and peripherin-labeled neurites travel along the OHCs in an unorganized pattern. (D-F) Both TMRD- and peripherin-labeled neurites formed three rows of outer spiral bundles beneath the OHCs in an organized pattern. The inner spiral plexus, associated with the IHCs, exhibited only TMRD labeling, but not peripherin labeling, at P3. (G-I) TMRD labeling was reduced under the OHCs compared with the strong representation of peripherin-expressing neurites in the outer spiral bundle region. Scale bars 10 μm. SGNI, type I spiral ganglion neurons; SGNII, type II spiral ganglion neurons.

intraganglionic spiral bundle (Fig. 1A,C, Fig. 2A, Fig. 3A,B). This is consistent with reports of the peripherin expression of SGN in the developing rat cochlea (Hafidi et al., 1993). The mid and basal turn regions of E18 cochlea showed an immature, unorganized innervation of both IHCs and OHCs by TMRD- and peripherin-labeled neurite populations (Fig. 3). Both afferent fiber types projected to the IHC region and extended beyond this, as neurites projecting to the OHC region (Fig. 3). The projecting neurites in the OHC region traveled short distances and formed contacts with few, predominantly first row, OHCs (Fig. 3B-D). The TMRD-labeled type I neurites innervating the IHCs had extensive terminals on the lateral walls of the cells (see Fig. S1 in the supplementary material), whereas the peripherin-positive type II fibers innervating the IHC had short terminal branches that were limited to the base of the cells. In the apical region at E18, few neurites of either type reached the inner spiral plexus region; there were no terminal processes on the IHCs and no fibers projecting to the OHCs (not shown).

Two days later, at P0, the distribution of the type I and type II SGNs within Rosenthal's canal was similar to E18 (data not shown), but the neurites of both these neuron populations showed more extensive projections to the IHCs and OHCs. Type I fiber innervation of the IHCs formed a calyceal meshwork of terminals around the base and lateral aspect of the cells, extending towards the cuticular plate region (Fig. 6B,E). There was a tendency for type I terminals to extend towards the medial aspect of the IHCs, with some extension of these projections to the adjacent inner phalangeal cells. TMRD-labeled fibers also projected to the three rows of OHCs, along with the peripherin-positive type II neurites (Fig. 4A-C, Fig. 6A,B,D,E), as the outer spiral bundles started to form with a divaricating innervation pattern. The visualization of TMRD- and peripherin-labeled neurites innervating both IHCs and OHCs at P0 (Fig. 6A,B,D,E) confirmed the transient innervation of type II SGNs to IHCs and type I to OHCs during cochlear synaptic reorganization (Perkins and Morest, 1975). At the apical turn, both types of neurites traveled only a short distance radially to contact small numbers of OHCs (data not shown), resembling the development of the cochlear innervation in the mid-basal regions between E18 and P0.

Afferent innervation at P3 represented the maximum overlap in neurite projections from type I and type II SGNs within the outer spiral bundles. Peripherin-expressing neurons were more frequently

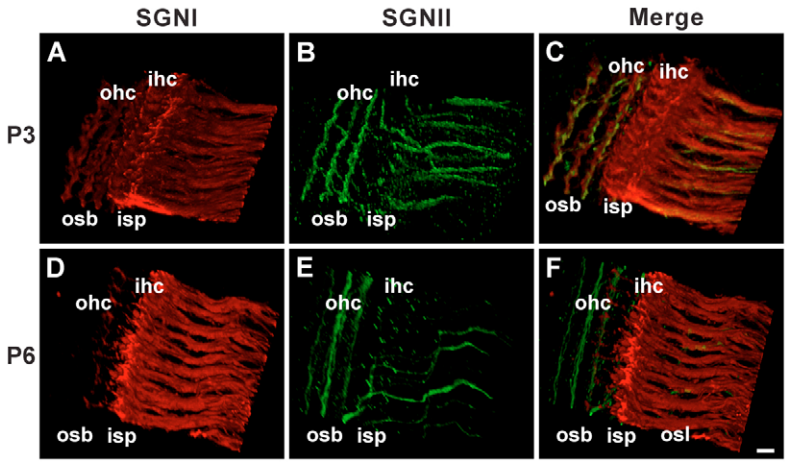

Fig. 5. Three-dimensional reconstruction of the afferent innervation in the organ of Corti at P3 and P6 in mice. Spatial resolution of the pathways for TMRD- (red) and peripherin- (green) labeled type I and type II neurites, respectively, under the hair cells. (**A-C**) At P3, both types of afferent nerve fibers were found under the OHCs, but their labeling was independent. TMRD labeling was found in the inner spiral plexus (ISP), forming a calyceal innervation to IHCs. In the outer spiral bundles (OSB) under the OHC, TMRD-labeled neurites were located above peripherin-immunopositive type II neurites in the hair cell region and osseous spiral lamina. (**D-F**) At P6, TMRD-labeled nerve fibers were largely confined to the ISP, with limited residual projection to the first row of OHCs. At this age, peripherin-labeled neurites formed three prominent rows of OSBs innervating the OHCs, after passing close to the basilar membrane below TMRD-labeled neurites. Scale bars: 10 μm. isp, inner spral plexus; osb, outer spiral bundle; osl, osseous spiral lamina; SGNI, type I spiral ganglion neurons; SGNII, type II spiral ganglion neurons.

found within the outer region of the spiral ganglion (Figs 4, 5), adjacent to the intraganglionic spiral bundle of efferent fibers. Peripherin-expressing type II neurites no longer branched to innervate IHCs collaterally by P3 (Figs 4, 5). However, TMRD-labeled neurites still formed a calyceal-type innervation to the IHCs, but with a more limited basolateral association (Fig. 4D-F, Fig. 5A-C, Fig. 6G,H,J,K). Unlike the type I SGN innervation to the inner spiral plexus region beneath the IHCs, both TMRD- and peripherin-labeled neurites continued to project to all three rows of OHCs, with the structure of the outer spiral bundles becoming well defined (Fig. 4D-F, Fig. 5A-C, Fig. 6G,H,J,K). Three-dimensional reconstructions of confocal images were utilized to provide spatial resolution of the growth path of the neurites under the hair cell region (Fig. 5). At P3, there was a lack of peripherin labeling in the inner spiral plexus and IHC region. At the outer spiral bundles, TMRD-labeled type I neurites lay above the peripherin-positive type II fibers, showing that they utilized different growth paths (Fig. 5A-C, Fig. 6G,H,J,K). TMRD-labeled neurites traveled in fascicles directed towards the organ of Corti, but peripherin-labeled neurites traveled as single fibers in a more diagonal orientation and often crossed beneath bundles of type I neurites. Both type I and type II neurites frequently coursed between outer spiral bundle fiber tracts (see Movie S1 in the supplementary material).

Discrimination of afferent and efferent fibers

The organ of Corti receives an extensive efferent innervation via the lateral olivocochlear input to the type I SGNs in the inner spiral plexus region and the medial olivocochlear bundle projection to the OHCs via tunnel-crossing fibers (Warr and Guinan, 1979). Our data indicate that once the mature innervation pattern is established, limited components of TMRD labeling may represent efferent fiber projections. This was primarily evident as weak intraganglionic spiral bundle and associated tunnel-crossing fiber labeling at P6 (Fig. 1A, Fig. 5D,F). These fibers were distinguishable from the type I SGN fibers by their trajectories in the organ of Corti. However, to specifically distinguish these fibers, we undertook ChAT immunolabeling of the cholinergic efferent fibers (Fig. 6C,F,I,L,O,R) (Merchan Perez et al., 1994; Sobkowicz and Emmerling, 1989). This established the profile of the efferent innervation in relation to the development of the afferent fiber populations in the mid-turn of the cochlea up to P6. There was no significant ChAT signal at P0 (Fig. 6C,F). At P3, very weak ChAT immunolabeling occurred in the inner spiral plexus region beneath the IHCs (Fig. 6I,L) and in the intraganglionic spiral bundle (data not shown). At P6, ChAT labeling of cholinergic efferent fibers was evident in the medial aspect of the inner spiral plexus beneath the IHCs (Fig. 6O,R). This was complemented by weak labeling of some tunnel-crossing fibers (medial olivocochlear bundle) extending to the OHCs. ChAT labeling was also present in the intraganglionic spiral bundle (not shown). We conclude therefore that between E18 and P6, the period of afferent synaptic reorganization in the cochlea, TMRD labeling resolved the type I SGN afferent innervation of the organ of Corti independent of the peripherin labeling of type II SGN and was distinguishable from the onset of efferent innervation.

DISCUSSION

Axon retraction and synapse elimination are required during early postnatal development to establish the correct wiring in the central and peripheral nervous systems (Walsh and Lichtman, 2003; Sugihara, 2006). During development of the cochlea, the IHCs and OHCs are innervated by two types of primary afferent neurons. However, in the adult, IHC and OHC innervation is reduced and these cells become exclusively innervated by type I and type II auditory nerve fibers, respectively, with additional complexity contributed by reciprocal synapses on the IHCs (Sobkowicz et al., 2003). Here, we have characterized in a way not previously possible how this mature innervation pattern becomes established. We have defined the development of afferent nerve innervation by visualizing the outgrowth, branching, pruning and withdrawal of the type I and type II afferent nerve fibers independently. This reorganization occurs at a crucial period in the development of the auditory system, just before the onset of hearing (around P10 in mice) (Kros et al., 1998).

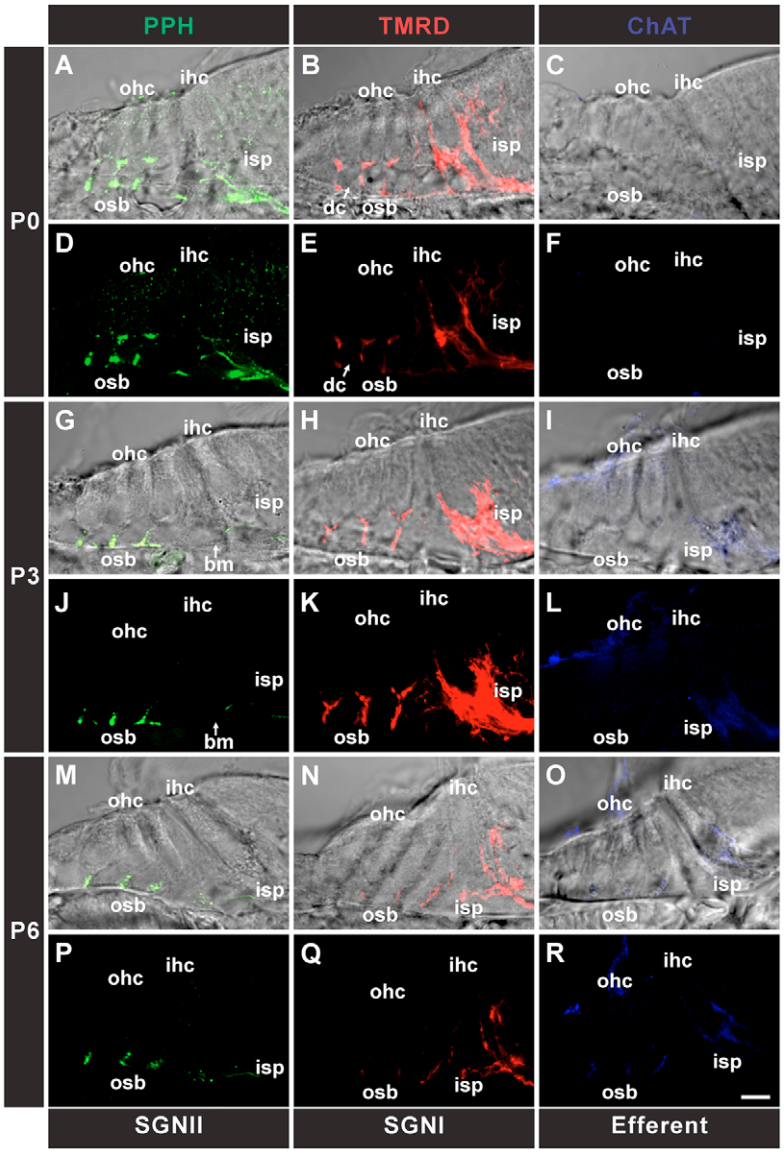

Fig. 6. TMRD, peripherin and ChAT labeling in the mouse organ of Corti between P0 and P6. Single confocal optical sections overlaid with (**A-C**,**G-I**,**M-O**) and without (**D-F**,**J-L**,**P-R**) transmitted-light images demonstrate the relationship between the labeled afferent and efferent nerve fibers and the cellular structures in the organ of Corti. (A-F) P0 organ of Corti showing peripherin- (green, type II SGNs) and TMRD- (red, type I SGNs) labeled neurites innervate both the IHCs and OHCs; no significant ChAT labeling was detected. (A,D) Peripherin-labeled type II neurites branch to innervate the IHCs, with primary neurite processes passing along the basilar membrane to innervate the three rows of OHCs. (B,E) Type I SGN fiber terminals make close contact with the basal and lateral membrane of the IHCs. (G-L) P3 organ of Corti shows both TMRD and peripherin labeling in the three rows of outer spiral bundles (OSBs); TMRD and ChAT labeling, but not peripherin labeling in the inner spiral plexus (ISP) under the IHCs. (G,J) Peripherin labeling is now absent under the IHCs. (H,K) TMRD labeling is more restricted to the basolateral region of the IHCs compared with P0 (see B,E). (I,L) Weak ChAT signal in the ISP. (M-R) Adult-like primary auditory afferent innervation pattern in the P6 organ of Corti with increased efferent nerve fiber labeling. (M,P) Peripherin-labeled neurites, as for P3, confined to the OSBs. (N,Q) TMRD-labeled neurites are predominantly found under the IHCs, while only minimal labeling was detected in the OSBs. Some TMRD-labeling would be attributed to efferent nerve fibers. (O,R) ChAT immunolabeling in both the ISP and OSBs. Scale bar: 10 μm. bm, basilar membrane; dc, Deiters' cell; isp, inner spral plexus; osb, outer spiral bundle; PPH, peripherin; SGNI, type I spiral ganglion neurons; SGNII, type II spiral ganglion neurons.

Stages of development of the afferent innervation of the organ of Corti

The direct visualization of developing innervation patterns from embryonic through postnatal development provided by this study has enabled the identification of three distinct stages of cochlear afferent innervation: (1) neurite growth and extension under the sensory hair cell region from both types of SGN between E18 and P0; (2) neurite refinement under OHCs from both types of SGN between P0 and P3; (3) neurite retraction of type I SGNs from OHCs and synaptic pruning between P3 and P6.

Neurite outgrowth and extension (E18-P0)

During this period, type I and type II SGN neurites project to the IHC and OHC regions and extend terminals towards the target hair cells. The signaling mechanism associated with this neurite outgrowth from the osseous spiral lamina is probably a result of neurotrophins, growth factors, morphogens, ephrins and/or semaphorins that are expressed in the developing inner ear and have been implicated in guiding auditory innervation (Rubel and Fritzsch, 2002; Webber and Raz, 2006). Significant evidence exists of roles for BDNF, NT3 (also known as NTF3 – Mouse Genome Informatics), semaphorin 3A and BRN3a (also known as POU4F1) (Huang et al., 2001; Coppola et al., 2001; Farinas et al., 2001; Gu et al., 2003; Fritzsch et al., 2005). BDNF probably plays the dominant role in this neurite outgrowth and extension stage, as multiple studies have shown BDNF to be the most important for short range guidance of SGN afferent fibers extending to hair cells (Pirvola et al., 1992; Wheeler et al., 1994; Coppola et al., 2001; Fritzsch et al., 2005). BDNF is expressed and released by the hair cells and attracts fiber outgrowth (Pirvola et al., 1992; Wheeler et al., 1994); however, as some fiber growth still occurs in the absence of hair cells, BDNF or sensory epithelia, directed afferent fiber outgrowth towards the target hair cells at this stage of development may also depend on matrix proteins such as semaphorins (Fritzsch et al., 2005).

Refinement of afferent fiber tracts and hair cell innervation (P0-P3)

The nerve fibers of both type I and type II SGNs are segregated into the three defined outer spiral bundles beneath the rows of OHCs. During this process, the type I SGN fiber tracts are separate, remaining dorsal to the type II SGN fiber tracts (see Movie S1 in the supplementary material; P3 organ of Corti innervation). In addition,

type I SGN innervation of the IHCs was refined, with calyceal terminal complexes forming around the basolateral region of these cells. These data provide the first resolution of the refinement of both the type I and type II afferent innervation to establish the outer spiral bundles, and the localization of synaptic terminals around the IHCs during this stage of afferent innervation. How fiber dominance is established is not known, but our finding that TMRD can specifically label type I fibers at this stage of development will enable future characterization of exclusively type I fiber synaptogenesis and refinement onto the IHCs.

Neurite retraction and synaptic pruning (P3-P6)

The excess of nerve terminals and associated ribbon synapses present at the OHCs is reduced to establish the mature innervation pattern (Sobkowicz et al., 1982; Pujol et al., 1998). This suggests that the type I afferent nerve fibers form synaptic contacts with the OHCs, which are then pruned, leading to withdrawal of this class of neurite from the OHC region. TMRD-labeling of type I fibers enabled us to directly visualize the type I fiber withdrawal from the OHCs (Figs 4-6). By contrast, the innervation pattern of the type II afferent nerve fibers is more stable and could be seen to supplant the type I innervation between P3 and P6 (Fig. 5). As the retraction is specific to type I fibers, this variation in type I versus type II stability at the OHCs probably results from distinct differences in the properties of the synaptic connections formed by the type I and type II fibers. The maturity and the molecular makeup of the temporary type I synapses onto the OHCs is currently unknown; however, glutamate receptors have been found to be expressed by type I fibers at this stage of development (Knipper et al., 1997; Eybalin et al., 2004), suggesting that these temporary synapses are at least capable of functional neurotransmission with the OHCs. We hypothesize that it is the molecular makeup of the temporary synapses that drives their retraction, with incomplete type I synapse formation onto the OHCs, resulting in an inability to compete against the stronger type II synapses. Direct competition for innervation is well characterized at the neuromuscular junction (Sanes and Lichtman, 2001; Lichtman and Sanes, 2003; Wyatt and Balice-Gordon, 2003) and may also occur in the inner ear. In addition, biochemical analysis has revealed that excitatory synapses in other brain regions express a myriad of proteins that play a pivotal role in targeting glutamate receptors to synapses and anchoring them at the postsynaptic density (Garner and Kindler, 1996; Montgomery et al., 2003). The differential expression of these postsynaptic density proteins at type I and type II synapses could play a crucial role in determining whether a synapse is temporary or stable and TMRD-labeling of type I fibers will enable future molecular characterization of the synapses formed by these fibers.

Changes in hair cell function during neurite retraction and synapse pruning may also contribute to variation in synaptic stability. For example, neonatal hair cells exhibit spontaneous action potentials, but during the period of neurite retraction this activity is lost as the membrane conductances mature in the early postnatal period (Kros et al., 1998; Housley et al., 2006).

Our recent data also suggest that ATP-gated ionotropic P2X receptor signaling contributes to neurite retraction (Greenwood et al., 2007). The expression of the $P2X_3$ subunits of ATP-gated ion channels in the SGNs is developmentally regulated and is closely coordinated with the cochlear afferent synaptic reorganization (Huang et al., 2005; Huang et al., 2006). P2X signaling was found to inhibit BDNF-induced neurite outgrowth and branching (Greenwood et al., 2007), suggesting that during the maturation of cochlear innervation, temporally regulated P2X receptor expression provides a potential mechanism to control BDNF-stimulated outgrowth when neurite pruning is required.

Development of type II fiber innervation

In the developing mouse cochlea, we found that peripherin was solely expressed by the type II SGNs from E18 onwards. This is in contrast to the developing rat cochlea, where peripherin is initially expressed in type I and type II SGNs and then downregulated early in the first postnatal week (Hafidi et al., 1993). Our data indicate that any expression of peripherin by type I SGNs would have to occur before E18 in the mouse. Multiple previous studies have shown anti-peripherin to exclusively stain type II neurons (Hafidi et al., 1993; Despres et al., 1994; Mou et al., 1998; Schimmang et al., 2003). We verified that our identification of type II fibers in the mouse was specific by replicating the peripherin labeling in the postnatal rat that was previously described by Hafidi et al. (Hafidi et al., 1993) (see Fig. S2 in the supplementary material). In our mouse tissue, 3D reconstructions show that TMRD- and peripherin-labeled fiber tracts were distinct within the osseous spiral lamina, outer spiral bundles and beneath the IHCs (see Movies S1 and S2 in the supplementary material). The majority of the peripherin-expressing neurites terminated on the OHCs during development, but between E18 and P0 some peripherin-positive nerve fibers formed a collateral innervation with the IHCs, supporting previous reports that type II SGNs temporarily project to IHCs during cochlear development (Perkins and Morest, 1975). Between E18 and P6, the number of peripherin-expressing neurons was decreased and redistributed towards the intraganglionic spiral bundles. This may be the result of cell migration and cell loss in the spiral ganglion during the first postnatal week, which rearranges and reduces the SGN II cell soma density in the ganglion, as has been evident in other species (Echteler and Nofsinger, 2000; Ard and Morest, 1984; Rueda et al., 1987). We also observed that the peripherin-expressing type II SGNs in the mid and basal turns were located mainly close to the lateral aspect of Rosenthal's canal, where the intraganglionic spiral bundle region is located. The number of type II SGNs gradually increased from the apical- to the mid-turn, consistent with previous studies (Spoendlin, 1972; Keithley and Feldman, 1979; Hafidi et al., 1993). These data, together with the findings of previous studies employing peripherin immunoreactivity (Hafidi et al., 1993; Despres et al., 1994; Mou et al., 1998; Schimmang et al., 2003), verify the use of peripherin to label type II SGNs and therefore provide a mechanism to independently identify the neurites of the type II SGN from the TMRD-labeled type I neurites.

Efferent innervation

Efferent fiber innervation patterns were visualized with ChAT immunolabeling (Sobkowicz and Emmerling, 1989; Merchan Perez et al., 1994). ChAT labeling verified that the TMRD-positive fibers examined during the neurite refinement and retraction stages were type I fibers and not efferent fibers. In the mid-turn, we observed no ChAT immunolabeling under the IHCs or OHCs until P3. By P6, some ChAT-positive efferent tunnel-crossing fibers were matched with limited TMRD labeling. ChAT-positive efferent fiber labeling in the region of the inner spiral plexus at P3 and P6 was lateral and basal to the TMRD-labeled SGN innervation of the hair cells. In addition to ChAT labeling, at P6 the efferent fibers could easily be distinguished by their unique travel path crossing the tunnel of Corti. TMRD-labeling of the efferent fibers in the mid-turn of the cochlea was not significant until P6, by which time the refinement and retraction of TMRD-labeled type I fibers was largely complete.

Our observed ChAT labeling is identical to that reported by Sobkowicz and Emmerling, (Sobkowicz and Emmerling, 1989), consistent with increased postnatal ChAT expression correlating with efferent synaptogenesis (Sobkowicz and Emmerling, 1989; Merchan Perez et al., 1994). Studies using DiI to characterize the development of efferent innervation (Fritzsch and Nichols, 1993; Bruce et al., 1997) show an earlier arrival of efferent nerve fibers in the organ of Corti: in the basal turn, DiI-labeled efferents could be seen extending to the OHCs by birth, lagging only slightly behind afferent innervation at the same stage (Bruce et al., 1997). Our observed absence of ChAT labeling in the mid-turn before P3 could be due to a lack of ChAT expression until after efferent nerve terminals are formed between P2 and P7 (Shnerson et al., 1982). However, examination of ChAT labeling in the basal turn revealed efferent fibers extending towards the inner hair cells at P0 (not shown), consistent with the timecourse from studies utilizing DiI labeling of efferents (Bruce et al., 1997) and with ChAT expression under the IHCs at the basal turn at P0 (Sobkowicz and Emmerling, 1989). Therefore, we believe that the lack of ChAT labeling we observed at P0 in the mid-turn is due to the basal-apical gradient, which can result in a lag in innervation of as much as 4 days. Our ChAT labeling provides an accurate picture of efferent innervation patterns and confirmed that up to P6, when the afferent neural innervation of the cochlea approached the mature configuration, TMRD labeling was able to specifically resolve the type I SGN innervation.

TMRD labeling of type I SGN

The TMRD-specific labeling of type I fibers has enabled for the first time the characterization of the developmental innervation patterns of type I and type II afferent fibers independently. The mechanism that allows TMRD to selectively label type I nerve fibers probably relates to the diameter of the nerve fibers that were sectioned to provide the dextran uptake pathway. The diameters of both type I SGNs (>1 μm) and cholinergic efferent fibers (~0.8 μm) are larger than for type II SGNs (<0.7 μm) in the adult mouse (Brown and Ledwith, 3rd, 1990; Wilson et al., 1991). We hypothesize that the smaller-diameter type II nerve fibers reseal before the dextran crystals can be taken up by these fibers. Additional potential mechanisms that underlie TMRD-specific labeling of type I fibers include a lower dextran diffusion efficiency in type II versus type I fibers due to a high density cytoskeletal meshwork in type II fibers (Schwartz et al., 1983; Dau and Wenthold, 1989). In addition, a higher dextran transport efficiency in the anterograde direction (Fritzsch, 1993; Kobbert et al., 2000) may have enabled TMRD labeling of efferent nerve fibers in the later stage of cochlear neural development.

Conclusions

Our data have defined the spatial and temporal development of cochlear afferent innervation by type I and type II SGN populations. We have identified three stages of the afferent innervation between E18 and P6: (1) neurite growth and extension of both classes of afferents to all the hair cells; (2) neurite refinement, with formation of the outer spiral bundles under OHCs; (3) neurite retraction and synaptic pruning to eliminate type I innervation of OHCs, while retaining their innervation of IHCs. These developmental stages are required to establish the mature cochlea innervation pattern. This precise spatiotemporal regulation of afferent nerve fiber development in the cochlea is probably to be associated with specific differences in the properties of the synapses formed by type I and II SGNs. The study also highlights the cochlea as a powerful model system for the study of synapse development, elimination and neurite retraction in the developing central nervous system.

We thank Dr Annie Wolf, Universite Pierre et Marie Curie, Paris for the peripherin antibody and Dr Fabiana Kubke for her advice on fast neural tracing techniques and comments on the manuscript. Supported by the Auckland Medical Research Foundation and Marsden Fund (Royal Society of New Zealand). Gary Housley is a James Cook Fellow (Royal Society of New Zealand). Lin-Chien Huang is a Deafness Research Foundation (NZ) doctoral scholarship recipient.

Supplementary material

Supplementary material for this article is available at http://dev.biologists.org/cgi/content/full/134/16/2925/DC1

References

Ard, M. D. and Morest, D. K. (1984). Cell death during development of the cochlear and vestibular ganglia of the chick. *Int. J. Dev. Neurosci.* **2**, 535-547.
Boyer, S., Ruel, J., Puel, J. L. and Chabbert, C. (2004). A procedure to label inner ear afferent nerve endings for calcium imaging. *Brain Res. Brain Res. Protoc.* **13**, 91-98.
Brown, M. C. and Ledwith, J. V., 3rd (1990). Projections of thin (type-II) and thick (type-I) auditory-nerve fibers into the cochlear nucleus of the mouse. *Hear. Res.* **49**, 105-118.
Bruce, L. L., Kingsley, J., Nichols, D. H. and Fritzsch, B. (1997). The development of vestibulocochlear efferents and cochlear afferents in mice. *Int. J. Dev. Neurosci.* **15**, 671-692.
Burda, H. and Branis, M. (1988). Postnatal development of the organ of Corti in the wild house mouse, laboratory mouse, and their hybrid. *Hear. Res.* **36**, 97-105.
Coppola, V., Kucera, J., Palko, M. E., Martinez-De Velasco, J., Lyons, W. E., Fritzsch, B. and Tessarollo, L. (2001). Dissection of NT3 functions in vivo by gene replacement strategy. *Development* **128**, 4315-4327.
Darrow, K. N., Maison, S. F. and Liberman, M. C. (2006). Cochlear efferent feedback balances interaural sensitivity. *Nat. Neurosci.* **9**, 1474-1476.
Darrow, K. N., Maison, S. F. and Liberman, M. C. (2007). Selective removal of lateral olivocochlear efferents increases vulnerability to acute acoustic injury. *J. Neurophysiol.* **97**, 1775-1785.
Dau, J. and Wenthold, R. J. (1989). Immunocytochemical localization of neurofilament subunits in the spiral ganglion of normal and neomycin-treated guinea pigs. *Hear. Res.* **42**, 253-263.
Despres, G., Leger, G. P., Dahl, D. and Romand, R. (1994). Distribution of cytoskeletal proteins (neurofilaments, peripherin and MAP-tau) in the cochlea of the human fetus. *Acta Otolaryngol.* **114**, 377-381.
Djabali, K., Portier, M. M., Gros, F., Blobel, G. and Georgatos, S. D. (1991). Network antibodies identify nuclear lamin B as a physiological attachment site for peripherin intermediate filaments. *Cell* **64**, 109-121.
Echteler, S. M. (1992). Developmental segregation in the afferent projections to mammalian auditory hair cells. *Proc. Natl. Acad. Sci. USA* **89**, 6324-6327.
Echteler, S. M. and Nofsinger, Y. C. (2000). Development of ganglion cell topography in the postnatal cochlea. *J. Comp. Neurol.* **425**, 436-446.
Eybalin, M., Caicedo, A., Renard, N., Ruel, J. and Puel, J. L. (2004). Transient Ca2+-permeable AMPA receptors in postnatal rat primary auditory neurons. *Eur. J. Neurosci.* **20**, 2981-2989.
Farinas, I., Jones, K. R., Tessarollo, L., Vigers, A. J., Huang, E., Kirstein, M., de Caprona, D. C., Coppola, V., Backus, C., Reichardt, L. F. et al. (2001). Spatial shaping of cochlear innervation by temporally regulated neurotrophin expression. *J. Neurosci.* **21**, 6170-6180.
Fritzsch, B. (1993). Fast axonal diffusion of 3000 molecular weight dextran amines. *J. Neurosci. Methods* **50**, 95-103.
Fritzsch, B. and Nichols, D. H. (1993). DiI reveals a prenatal arrival of efferents at the differentiating otocyst of mice. *Hear. Res.* **65**, 51-60.
Fritzsch, B., Pauley, S., Matei, V., Katz, D. M., Xiang, M. and Tessarollo, L. (2005). Mutant mice reveal the molecular and cellular basis for specific sensory connections to inner ear epithelia and primary nuclei of the brain. *Hear. Res.* **206**, 52-63.
Garner, C. C. and Kindler, S. (1996). Synaptic proteins and the assembly of synaptic junctions. *Trends Cell Biol.* **6**, 429-433.
Gimlich, R. L. and Braun, J. (1985). Improved fluorescent compounds for tracing cell lineage. *Dev. Biol.* **109**, 509-514.
Glover, J. C., Petursdottir, G. and Jansen, J. K. (1986). Fluorescent dextran-amines used as axonal tracers in the nervous system of the chicken embryo. *J. Neurosci. Methods* **18**, 243-254.
Greenwood, D., Jagger, D. J., Huang, L.-C., Hoya, N., Thorne, P. R., Wildman, S. S., King, B. F., Pak, K., Ryan, A. F. and Housley, G. D. (2007). P2X receptor signaling inhibits BDNF-mediated spiral ganglion neuron development in the neonatal rat cochlea. *Development* **134**, 1407-1417.

Gu, C., Rodriguez, E. R., Reimert, D. V., Shu, T., Fritzsch, B., Richards, L. J., Kolodkin, A. L. and Ginty, D. D. (2003). Neurophilin-1 conveys semaphorin and VEGF signaling during neural and cardiovascular development. *Dev. Cell* **5**, 45-57.
Hafidi, A. (1998). Peripherin-like immunoreactivity in type II spiral ganglion cell body and projections. *Brain Res.* **805**, 181-190.
Hafidi, A., Despres, G. and Romand, R. (1993). Ontogenesis of type II spiral ganglion neurons during development: peripherin immunohistochemistry. *Int. J. Dev. Neurosci.* **11**, 507-512.
Housley, G. D., Marcotti, W., Navaratnam, D. and Yamoah, E. N. (2006). Hair cells–beyond the transducer. *J. Membr. Biol.* **209**, 89-118.
Huang, E. J., Liu, W., Fritzsch, B., Bianchi, L. M., Reichardt, L. F. and Xiang, M. (2001). Brn3a is a transcriptional regulator of soma size, target field innervation and axon path finding of inner ear sensory neurons. *Development* **128**, 2421-2432.
Huang, L. C., Greenwood, D., Thorne, P. R. and Housley, G. D. (2005). Developmental regulation of neuron-specific P2X3 receptor expression in the rat cochlea. *J. Comp. Neurol.* **484**, 133-143.
Huang, L. C., Ryan, A. F., Cockayne, D. A. and Housley, G. D. (2006). Developmentally regulated expression of the P2X(3) receptor in the mouse cochlea. *Histochem. Cell Biol.* **125**, 681-692.
Jagger, D. J. and Housley, G. D. (2003). Membrane properties of type II spiral ganglion neurones identified in a neonatal rat cochlear slice. *J. Physiol.* **552**, 525-533.
Kaneko, T., Saeki, K., Lee, T. and Mizuno, N. (1996). Improved retrograde axonal transport and subsequent visualization of tetramethylrhodamine (TMR) –dextran amine by means of an acidic injection vehicle and antibodies against TMR. *J. Neurosci. Methods* **65**, 157-165.
Keithley, E. M. and Feldman, M. L. (1979). Spiral ganglion cell counts in an age-graded series of rat cochleas. *J. Comp. Neurol.* **188**, 429-442.
Keithley, E. M. and Feldman, M. L. (1982). Hair cell counts in an age-graded series of rat cochleas. *Hear. Res.* **8**, 249-262.
Knipper, M., Kopschall, I., Rohbock, K., Kopke, A. K., Bonk, I., Zimmermann, U. and Zenner, H. (1997). Transient expression of NMDA receptors during rearrangement of AMPA-receptor-expressing fibers in the developing inner ear. *Cell Tissue Res.* **287**, 23-41.
Kobbert, C., Apps, R., Bechmann, I., Lanciego, J. L., Mey, J. and Thanos, S. (2000). Current concepts in neuroanatomical tracing. *Prog. Neurobiol.* **62**, 327-351.
Kros, C. J., Ruppersberg, J. P. and Rusch, A. (1998). Expression of a potassium current in inner hair cells during development of hearing in mice. *Nature* **394**, 281-284.
Lenoir, M., Shnerson, A. and Pujol, R. (1980). Cochlear receptor development in the rat with emphasis on synaptogenesis. *Anat. Embryol.* **160**, 253-262.
Lichtman, J. W. and Sanes, J. R. (2003). Watching the neuromuscular junction. *J. Neurocytol.* **32**, 767-775.
Malenka, R. C. (2003). The long-term potential of LTP. *Nat. Neurosci. Rev.* **4**, 923-926.
Merchan Perez, A., Gil-Loyzaga, P., Eybalin, M., Fernandez Mateos, P. and Bartolome, M. V. (1994). Choline-acetyltransferase-like immunoreactivity in the organ of Corti of the rat during postnatal development. *Brain Res. Dev. Brain Res.* **82**, 29-34.
Montgomery, J. M. and Madison, D. V. (2004). Discrete synaptic states define a major mechanism for synaptic plasticity. *Trends Neurosci.* **27**, 744-750.
Montgomery, J. M., Zamorano, P. and Garner, C. C. (2003). MAGUKs in synapse assembly and function: an emerging view. *Cell. Mol. Life Sci.* **61**, 911-929.
Mou, K., Adamson, C. L. and Davis, R. L. (1998). Time-dependence and cell-type specificity of synergistic neurotrophin actions on spiral ganglion neurons. *J. Comp. Neurol.* **402**, 129-139.
Oster, S. F. and Sretavan, D. W. (2003). Connecting the eye to the brain: the molecular basis of ganglion cell axon guidance. *Br. J. Ophthalmol.* **87**, 639-645.
Perkins, R. E. and Morest, D. K. (1975). A study of cochlear innervation patterns in cats and rats with the Golgi method and Nomarkski Optics. *J. Comp. Neurol.* **163**, 129-158.
Pickles, J. (1988). *An Introduction to the Physiology of Hearing*. London: Academic Press.
Pirvola, U., Ylikoski, J., Palgi, J., Lehtonen, E., Arumae, U. and Saarma, M. (1992). Brain-derived neurotrophic factor and neurotrophin 3 mRNAs in the peripheral target fields of developing inner ear ganglia. *Proc. Natl. Acad. Sci. USA* **89**, 9915-9919.
Popov, S. and Poo, M. M. (1992). Diffusional transport of macromolecules in developing nerve processes. *J. Neurosci.* **12**, 77-85.
Pujol, R., Lavigne-Rebillard, M. and Lenoir, M. (1998). Development of sensory and neural structures in the mammalian cochlea. In *Development of the Auditory System* (ed. E. W. Rubel, A. N. Popper and R. R. Fay), pp. 146-192. New York: Springer.
Roth, B. and Bruns, V. (1992a). Postnatal development of the rat organ of Corti. I. General morphology, basilar membrane, tectorial membrane and border cells. *Anat. Embryol.* **185**, 559-569.
Roth, B. and Bruns, V. (1992b). Postnatal development of the rat organ of Corti. II. Hair cell receptors and their supporting elements. *Anat. Embryol.* **185**, 571-581.
Rubel, E. W. and Fritzsch, B. (2002). Auditory system development: primary auditory neurons and their targets. *Annu. Rev. Neurosci.* **25**, 51-101.
Ruben, R. J. (1967). Development of the inner ear of the mouse: a radioautographic study of terminal mitoses. *Acta Otolaryngol. Suppl.* **220**, 1-44.
Rueda, J., de la Sen, C., Juiz, J. M. and Merchan, J. A. (1987). Neuronal loss in the spiral ganglion of young rats. *Acta Otolaryngol.* **104**, 417-421.
Sanes, J. R. and Lichtman, J. W. (2001). Induction, assembly, maturation and maintenance of a postsynaptic apparatus. *Nat. Rev. Neurosci.* **2**, 791-805.
Schimmang, T., Tan, J., Muller, M., Zimmermann, U., Rohbock, K., Kopschall, I., Limberger, A., Minichiello, L. and Knipper, M. (2003). Lack of Bdnf and TrkB signalling in the postnatal cochlea leads to a spatial reshaping of innervation along the tonotopic axis and hearing loss. *Development* **130**, 4741-4750.
Schwartz, A. M., Parakkal, M. and Gulley, R. L. (1983). Postnatal development of spiral ganglion cells in the rat. *Am. J. Anat.* **167**, 33-41.
Shnerson, A., Devigne, C. and Pujol, R. (1982). Age-related changes in the C57BL/6J mouse cochlea. II. Ultrastructural findings. *Dev. Brain Res.* **2**, 77-88.
Simmons, D. D. (1994). A transient afferent innervation of outer hair cells in the postnatal cochlea. *NeuroReport* **5**, 1309-1312.
Slepecky, N. B. (1996). Structure of the mammalian cochlea. In *The Cochlea* (ed. P. Dallos, A. N. Popper and R. R. Fay), pp. 44-129. New York: Springer.
Sobkowicz, H. M. and Emmerling, M. R. (1989). Development of acetylcholinesterase-positive neuronal pathways in the cochlea of the mouse. *J. Neurocytol.* **18**, 209-224.
Sobkowicz, H. M., Rose, J. E., Scott, G. E. and Slapnick, S. M. (1982). Ribbon synapses in the developing intact and cultured organ of Corti in the mouse. *J. Neurosci.* **2**, 942-957.
Sobkowicz, H. M., Slapnick, S. M. and August, B. K. (2003). Reciprocal synapses between inner hair cell spines and afferent dendrites in the organ of corti of the mouse. *Synapse* **50**, 53-66.
Spoendlin, H. (1972). Innervation densities of the cochlea. *Acta Otolaryngol.* **73**, 235-248.
Sugihara, I. (2006). Organization and remodeling of the olivocerebellar climbing fiber projection. *Cerebellum* **5**, 15-22.
Terao, E., Janssens, S., van den Bosch de Aguilar, P., Portier, M. and Klosen, P. (2000). In vivo expression of the intermediate filament peripherin in rat motoneurons: modulation by inhibitory and stimulatory signals. *Neuroscience* **101**, 679-688.
Walsh, M. K. and Lichtman, J. W. (2003). In vivo time-lapse imaging of synaptic takeover associated with naturally occurring synapse elimination. *Neuron* **37**, 67-73.
Warr, W. B. and Guinan, J. J., Jr (1979). Efferent innervation of the organ of corti: two separate systems. *Brain Res.* **173**, 152-155.
Webber, A. and Raz, Y. (2006). Axon guidance cues in auditory development. *Anat. Rec. A Discov. Mol. Cell. Evol. Biol.* **288**, 390-399.
Wheeler, E. F., Bothwell, M., Schecterson, L. C. and von Bartheld, C. S. (1994). Expression of BDNF and NT-3 mRNA in hair cells in the organ of Corti: quantitative analysis in developing rats. *Hear. Res.* **73**, 46-56.
Wilson, J. L., Henson, M. M. and Henson, O. W., Jr (1991). Course and distribution of efferent fibers in the cochlea of the mouse. *Hear. Res.* **55**, 98-108.
Wyatt, R. M. and Balice-Gordon, R. J. (2003). Activity-dependent elimination of neuromuscular synapses. *J. Neurocytol.* **32**, 777-794.